

Induced Alignment of a Solution-Cast Discotic Hexabenzocoronene Derivative for Electronic Devices Investigated by Surface X-ray Diffraction

Oliver Bunk,^{*} Martin M. Nielsen,[†] Theis I. Sølling,[†] Anick M. van de Craats,^{‡,§} and Natalie Stutzmann^{‡,||}

Contribution from the Materials Research Department and Danish Polymer Centre, Risø National Laboratory, P.O. Box 49, 4000 Roskilde, Denmark and Department of Physics, Cavendish Laboratory, Optoelectronics Group, University of Cambridge, Madingley Road, CB3 0HE Cambridge, United Kingdom

Received September 11, 2002; E-mail: Oliver.Bunk@risoe.dk

Abstract: A surface X-ray diffraction study is presented showing that highly ordered and uniaxially aligned hexa(3,7-dimethyl-octanyl)hexa-peri-hexabenzocoronene (HBC-C8,2) films can be fabricated by crystallization from solution onto friction-transferred poly(tetrafluoroethylene) (PTFE) layers. Three crystalline HBC-C8,2 majority phases result. In all three phases, the HBC-C8,2 molecules self-organize into columns which are uniaxially aligned along the direction defined by the PTFE macromolecules of the substrate. The three phases are quite similar, the major difference being their orientation with respect to the substrate. A quasi-2D epitaxial growth mechanism with a grapho-epitaxial component for one of the three phases explains the formation of the three rotational HBC-C8,2 variants. A method to obtain a thin film with only one phase is proposed. The results show that standard Θ - 2Θ X-ray diffraction and transmission electron diffraction can be very misleading tools to estimate the crystalline quality in a thin film of complex structure.

Introduction

A major challenge in the fabrication of efficient (opto-)electronic devices is to control the structural order and the alignment of the ordered units of the preferably solution-processed active semiconductor material, as this can improve charge carrier transport in the material significantly.^{1,2} A promising way appears to be exploiting the ability of organic molecules to self-organize. In addition, adequate substrates might be employed, to provide nucleation sites and thereby induce a certain alignment. Especially, highly oriented poly(tetrafluoroethylene) (PTFE) layers have been found to be a useful tool for the alignment of many organic compounds.

PTFE Friction-Transfer Layers. Sliding a PTFE rod at low speed and moderately high temperature over a clean glass slide yields a highly oriented thin film, as already reported in 1964 in a comprehensive study of the friction properties of PTFE.³ By electron diffraction, it was determined that the helical

molecular chains are oriented parallel to the sliding direction and form a hexagonal array with an interchain spacing of ~ 5.7 Å. In 1991, it was reported that these PTFE friction-transfer layers orient a wide variety of materials.⁴ In fact, they are often superior to other friction-transfer layers.⁵ Also, the attempt to replace PTFE substrates by rubbed polyimide was not successful in the case of several semicrystalline polymers,⁶ which further illustrates the uniqueness of PTFE friction-transfer layers as a substrate.

PTFE friction-transfer layers orient a broad variety of materials; more than one would intuitively expect. For example, simple lattice matching arguments often do not apply. Atomic force microscopy measurements show that the surface of such friction-transfer layers of PTFE molecules (molecular length of ~ 30 μm) is made up of ridges with a height typically of 1–50 nm and a spacing of < 25 nm to > 1 μm , with extended molecularly flat areas between the ridges.^{7,8} Taking this into account, one may assume that grapho-epitaxial growth with the nucleation at structural irregularities such as defects and steps – rather than epitaxial growth, that is, the commensurate growth mode with thin film and substrate structure in registry – explains

^{*} Materials Research Department, Risø National Laboratory.

[†] Danish Polymer Centre, Risø National Laboratory.

[‡] University of Cambridge.

[§] Present address: Netherlands Forensic Institute (NFI), Volmerlaan 17, 2288 GD Rijswijk, The Netherlands.

^{||} Present address: Philips Research, Prof. Holstlaan 4, NL-5656 AA Eindhoven, The Netherlands.

- (1) Siringhaus, H.; Wilson, R. J.; Friend, R. H.; Inbasekaran, M.; Wu, W.; Woo, E. P.; Grell, M.; Bradley, D. D. C. *Appl. Phys. Lett.* **2000**, *77*, 406–408.
- (2) Siringhaus, H.; Brown, P. J.; Friend, R. H.; Nielsen, M. M.; Bechgaard, K.; Langeveld-Voss, B. M. W.; Spiering, A. J. H.; Janssen, R. A. J.; Meijler, E. W.; Herwig, P.; de Leeuw, D. M. *Nature* **1999**, *401*, 685–688.
- (3) Makinson, K. R.; Tabor, D. *Proc. R. Soc. London, Ser. A* **1964**, *281*, 49–61.

(4) Wittmann, J. C.; Smith, P. *Nature* **1991**, *352*, 414–417.

(5) Motamedi, F.; Ihn, K. J.; Fenwick, D.; Wittmann, J. C.; Smith, P. *J. Polym. Sci., Part B: Polym. Phys.* **1994**, *32*, 453–457.

(6) Krüger, J. K.; Heydt, B.; Fischer, C.; Baller, J.; Jiménez, R.; Bohn, K.-P.; Servet, B.; Galtier, P.; Pavel, M.; Ploss, B.; Beghi, M.; Bottani, C. *Phys. Rev. B* **1997**, *55*, 3497–3506.

(7) Hansma, H.; Motamedi, F.; Smith, P.; Hansma, P.; Wittmann, J. C. *Polymer* **1992**, *33*, 647–649.

(8) Fenwick, D.; Smith, P.; Wittmann, J. C. *J. Mater. Sci.* **1996**, *31*, 128–131.

the alignment capabilities of PTFE layers. However, for vapor deposition of titanyl phthalocyanine on oriented PTFE substrates, a more complex mechanism involving a grapho-epitaxial coalescence along the PTFE macrosteps followed by a reorganization of amorphous aggregates into microcrystallites has been proposed.⁹ For vapor deposited diazo-dyes on PTFE, it has been found that slight modifications of the molecular structure lead to significant changes in the orientational ordering.¹⁰ This would be surprising in the case of grapho-epitaxial growth. Indeed, on the basis of molecular dynamics calculations and UV-vis absorption spectroscopy, it has been proposed that the grooves between adjacent PTFE chains orient the dye molecules,¹¹ resulting in at least one-dimensional (1D) epitaxial growth of the thin film. In the case of vacuum deposited tris(8-hydroxyquinoline) aluminum(III) (Alq), it has been found that, additional to microcrystallites oriented along the PTFE sliding direction, also crystallites oriented under an angle of $\pm 60^\circ$ with respect to this direction occur. This was explained by a 1D epitaxy mechanism which selects the fast growth directions.¹² At any rate, there is a multitude of examples for both molecular epitaxial and grapho-epitaxial growth, and in general, the two mechanisms may operate in conjunction.⁸

A major part of the previous structural studies of organic thin films have focused on conventional vacuum deposition on different substrates. The advantage of this technique is the good control over the experimental parameters, which allows the investigation of “clean”, well-defined model systems. However, vacuum deposition is often costly and high temperatures are commonly required. By contrast, for commercial exploitation, it would be most desirable to rely on simple, straightforward solution processes.

Discotic Materials, HBC-C8,2. In the search for organic materials which are suitable for electronic devices, discotic materials receive an increasing amount of attention. The flat, aromatic cores of discotic materials with their flexible side groups promote the self-organization of the molecules into columnar stacks, which can be seen as an example of micro-segregation.¹³ Dependent on the specific core and the peripheral substitution pattern, these materials very often exhibit a liquid crystalline phase (called D_h or Col_h) over an extended temperature range. In this D_h phase, the columnar arrangement is still preserved. Crystalline (K) derivatives of hexabenzocoronene (HBC) exhibit a high intrinsic charge carrier mobility in excess of $1 \text{ cm}^2 \text{ V}^{-1} \text{ s}^{-1}$, as determined by pulse-radiolysis time-resolved microwave conductivity.¹⁴ The efficient charge transport pathway is preserved in the liquid crystalline phase, and a mobility value as high as $0.5 \text{ cm}^2 \text{ V}^{-1} \text{ s}^{-1}$ was found.¹⁴ The HBC cores peripherally substituted with six hydrocarbon chains and stacked into columns can be seen as a coaxial conductor, in which the charge transport is enabled because of the overlap of the extended π -orbitals of the HBC cores. This conducting region is insulated by the hydrocarbon chains. The hydrocarbon chains render the molecules soluble and thereby enable processing in solution like spin-coating and solution-casting. An

advantage of low molecular weight components is that they are usually easier to purify from solution than polymers.

Efficient use of the high intrinsic charge carrier mobility of HBCs requires uniaxial alignment of the “coaxial conductors”, that is, the columnar stacks. PTFE friction-transfer layers recently were shown to be an excellent substrate for aligning HBC derivatives,¹⁵ such as the hexa(3,7-dimethyl-octanyl)hexa-peri-hexabenzocoronene (HBC-C8,2), which enabled the fabrication of thin film field-effect transistors (FETs) with HBC-C8,2 on PTFE as the active layer. These HBC-C8,2 devices with the channel parallel to the aligned columnar stacks were found to display a clear gate modulation (i.e., clear field effect), high on-off ratios of 10^4 , and for organic materials reasonably high field-effect mobilities, μ_{\parallel} , of up to $10^{-3} \text{ cm}^2 \text{ V}^{-1} \text{ s}^{-1}$ have been recorded.¹⁵ In contrast, for devices of the same configuration but based on aligned films with the columns perpendicular to the channel, and for isotropic HBC-C8,2 layers fabricated by spin-coating, markedly lower source-drain currents were measured, and thus, no distinct field effect could be observed. The mobilities μ_{\perp} and μ_{iso} could only be estimated. They are at least 2 orders of magnitude lower than μ_{\parallel} , which unambiguously illustrates the strong dependence of device properties from the discotic film morphology. Thus, deeper insight in the origin of the PTFE-nucleated, highly oriented crystal growth processes and mechanisms is highly desirable and will be of paramount importance to improve the FET performance even further. In fact, the field-effect mobilities μ_{\parallel} obtained for aligned HBC-C8,2 films are still below the intrinsic mobilities, as determined by microwave conductivity measurements ($\mu_{\text{intrinsic}} = 0.4 \text{ cm}^2 \text{ V}^{-1} \text{ s}^{-1}$). The determination of the structure, nucleation mechanism, and growth mode of HBC-C8,2 on PTFE layers provides the basis for understanding this behavior and finding ways to enhance the charge-carrier mobility. These problems are approached in a series of surface X-ray diffraction (SXRD) experiments.

Experimental Section

HBC-C8,2/PTFE. Hexa(3,7-dimethyl-octanyl)hexa-peri-hexabenzocoronene (HBC-C8,2) was synthesized by Müllen et al.¹⁶ The PTFE friction-transfer layers were prepared by sliding a PTFE rod at a constant speed of 0.1 mm/s over a clean glass substrate. The pressure applied to the rod was 5 kg/cm^2 , and the temperature of the substrate, 300°C . Typical PTFE layer thicknesses are reported to be in the range from 15 to 40 nm.^{7,8} Thin HBC-C8,2 films of 50–100 nm were produced by drying a droplet of $\sim 6 \text{ mg/ml}$ cyclohexanone solution between two PTFE coated glass slides.

SXRD Experiment. The thin films were investigated as prepared on their glass substrate; in surface X-ray diffraction (SXRD) investigations, it is not necessary to peel the film of the substrate as it has to be done for transmission electron diffraction measurements. Hence, the samples closely resemble actual FET devices.

The SXRD measurements were performed using the z-axis diffractometer at the wiggler beamline BW2¹⁷ at the Hamburger Synchrotronstrahlungslabor (HASYLAB). A monochromatic beam of 10 keV corresponding to a wavelength of $\lambda = 1.2398 \text{ \AA}$ impinged on the sample surface under a grazing angle of 0.16° . This angle of incidence lies between the critical angles for total reflection of the thin HBC-C8,2

(9) Brinkmann, M.; Wittmann, J.-C.; Barthel, M.; Hanack, M.; Chaumont, C. *Chem. Mater.* **2002**, *14*, 904–914.

(10) Tanaka, T.; Honda, Y.; Ishitobi, M. *Langmuir* **2001**, *17*, 2192–2198.

(11) Tanaka, T.; Ishitobi, M. *J. Phys. Chem. B* **2002**, *106*, 564–569.

(12) Moulin, J.-F.; Brinkmann, M.; Thierry, A.; Wittmann, J.-C. *Adv. Mater.* **2002**, *14*, 436–439.

(13) Tschierske, C. *Annu. Rep. Prog. Chem., Sect. C* **2001**, *97*, 191–267.

(14) van de Craats, A. M.; Warman, J. M.; Fechtenkötter, A.; Brand, J. D.; Harbison, M. A.; Müllen, K. *Adv. Mater.* **1999**, *11*, 1469–1472.

(15) van de Craats, A. M.; Stutzmann, N.; Bunk, O.; Nielsen, M. M.; Watson, M.; Müllen, K.; Chancy, H. D.; Sirringhaus, H.; Friend, R. H. *Adv. Mater.*, accepted for publication.

(16) Müller, M.; Kübel, C.; Müllen, K. *Chem.—Eur. J.* **1998**, *4*, 2099–2109.

(17) Drube, W.; Schulte-Schrepping, H.; Schmidt, H.-G.; Treusch, R.; Materlik, G. *Rev. Sci. Instrum.* **1995**, *66*, 1668–1670.

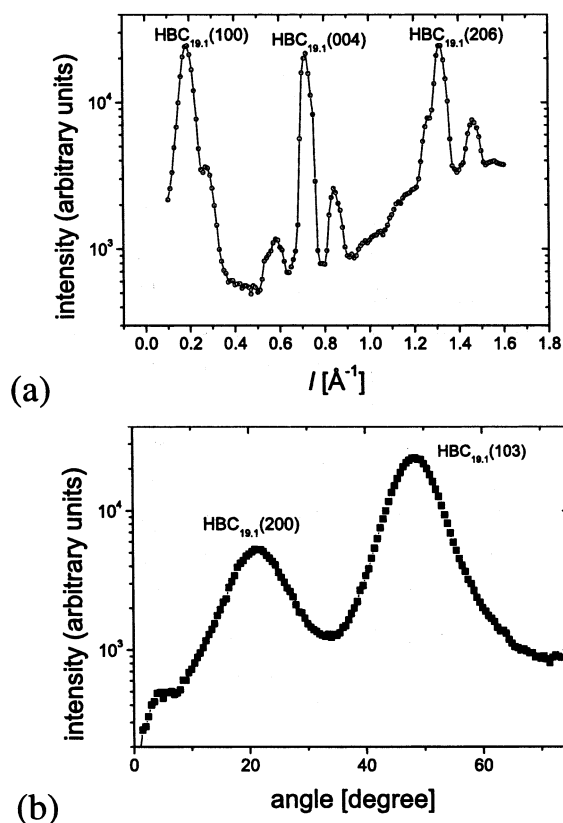


Figure 1. Examples of surface X-ray diffraction data. (a) Rod scan at a fixed (h,k) position along l . Shown is the $(0.258,0,l)$ rod. (b) Circle scan at constant momentum transfer. Shown is the scan in the (h,l) plane at $\mathbf{q} = \sqrt{h^2+l^2} = 0.653 \text{ \AA}^{-1} = 2\pi/(19.2/2) \text{ \AA}$.

film and of the glass substrate. It was chosen to maximize the measured signal, to minimize the background in the measurements, and to prevent radiation damage. The sample was kept in a helium atmosphere to further lower background scattering and radiation damage. A scintillation detector was used for the measurements. According to the standard z -axis design,^{18,19} the detector has two rotational degrees of freedom and the sample rotation provides an additional degree of freedom. The reciprocal space was systematically explored, for example, in line scans parallel to the surface plane, in line scans perpendicular to the surface plane along the crystal-truncation rods (CTRs),²⁰ and in circle scans at constant momentum transfer (i.e., constant length of the scattering vector \mathbf{q}). Examples of typical scans are shown in Figure 1. The precise position of most of the peaks observed in these scans and thereby the corresponding scattering vector \mathbf{q} was determined by iteratively rotating the detector and sample.

SXRD Data Analysis. The repeat distance d in the direct space probed by a diffraction peak is obtained with the relationship $d = 2\pi/q$ from the length of the scattering vector. The direction in which d is probed is defined by the vector character of the scattering vector. Higher orders with multiples of the first-order reflection scattering vector should be found for strong reflections. Also, if high symmetry directions are probed, systematic extinctions of reflections may occur. If a sufficient number of reflections is recorded, the unit cell(s) of the ordered phase(s) can be determined. A considerable higher number of reflections is necessary to perform a full 3D structure determination which includes the determination of all atom positions. For organic thin films, this is normally difficult, since the crystalline quality usually does not suffice and since not enough diffraction peaks are observable. However, a full

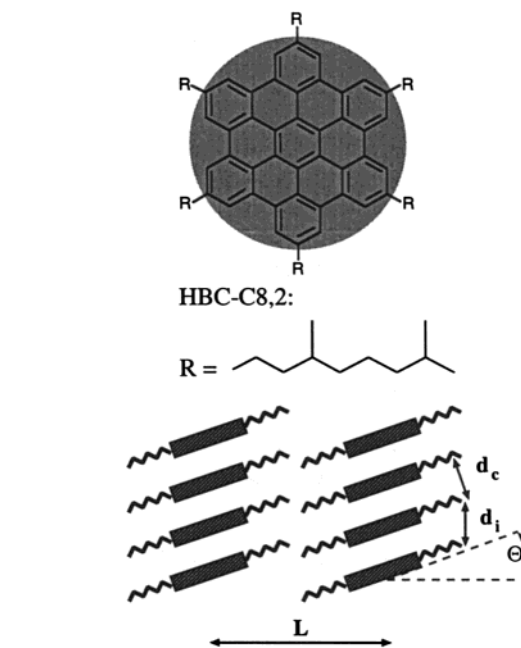


Figure 2. (Top) Hexabenzocoronene (HBC) is a molecule with a flat, disklike aromatic core. HBC-C8,2 is peripherally substituted with six branched side chains. (Bottom) Schematic representation of the HBC-C8,2 columns. The cofacial distance d_c is usually around 3.4 \AA . The intracolumnar distance d_i , which is related to the tilt Θ of the columns via $d_i = d_c/\cos(\Theta)$, is 5.2 \AA for HBC-C8,2. For HBC-C8,2, a typical intercolumnar distance L of 20 \AA was found.

3D structure determination is not necessary, if the basic chemical structure of the molecules is known, as is the case for HBC-C8,2. The determination of the dimension(s) and orientation(s) of the unit cell(s) and the symmetry properties of the molecular arrangement(s) within the unit cell(s) provide valuable information about the nanoscale structure, as discussed in the following section.

Results and Discussion

A model with three crystalline HBC-C8,2 majority phases consistently explains all Bragg peaks at which strong intensity was observed. The three HBC-C8,2 phases, denoted HBC_{0°}, HBC_{19.1°}, and HBC_{35.2°}, have the same basic structure, as described in the following. Each phase consists of HBC-C8,2 columns running parallel to the PTFE chains of the substrate. No evidence was found for columns standing perpendicular to the surface. Some disorder along the columns is evident from the damping of the diffracted intensity at positions which are sensitive to intracolumnar distances along the columns. Nevertheless, the repeat distance along the columns can be deduced to be 5.2 \AA , since only peaks corresponding to this distance are found. Assuming that the molecular cores keep a distance of 3.4 \AA , we can derive a tilt angle of $\arccos(3.4/5.2) \approx 49^\circ$ (Figure 2). Such a tilt is very close to the tilt in unsubstituted bulk HBC of 48° .²¹

2D Unit Cell. Because of the missing long-range order along the HBC-C8,2 columns, most of the data obtained contain structural information only about a 2D cut perpendicular to the HBC-C8,2 columns. The three phases found are shown in such a cross section in Figure 3. The observed 2D unit cell is rectangular. The SXRD data can accommodate a deviation of up to 1° from right angles. The longer side of the unit cell is by

(18) Feidenhans'l, R. *Surf. Sci. Rep.* **1989**, *10*, 105–188.

(19) Bloch, J. M. *J. Appl. Crystallogr.* **1985**, *18*, 33–36.

(20) Robinson, I. K. *Phys. Rev. B* **1986**, *33*, 3830–3836.

(21) Goddard, R.; Haenel, M. W.; Herndon, W. C.; Krüger, C.; Zander, M. *J. Am. Chem. Soc.* **1995**, *117*, 30–41.

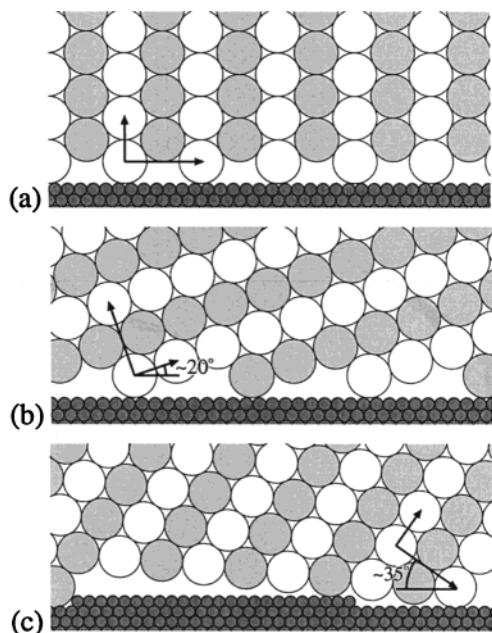


Figure 3. Structural models for the three observed HBC-C8,2 phases in a side view along the tilted HBC-C8,2 columns and the PTFE chains, perpendicular to the sample surface. The HBC-C8,2 cores are assumed to be tilted by $\sim 49^\circ$ (the tilt direction was not directly determined; therefore, the columns are indicated by circles, not by ellipses). The 2D unit cells are indicated by arrows. The three phases are (a) HBC $_0^\circ$, (b) HBC $_{19.1^\circ}$, and (c) HBC $_{35.2^\circ}$.

a factor of $\sqrt{3}$ longer than the short side, as one would expect for hexagonal packing. The short unit cell side has a length of around 20 Å. For a hexagonal arrangement, this length corresponds to the intercolumnar distance L . The two columns in the unit cell are not completely equivalent, and the columnar packing can therefore only be called quasi-hexagonal. The observed symmetry considerably restricts the number of structures compatible with the data: In a projection on the long axis of the unit cell, the two HBC-C8,2 columns are equivalent and evenly spaced, whereas, in a projection on the short axis of the unit cell, these two columns are inequivalent. This finding is compatible with a glide-line symmetry with the glide mirror line parallel to the long axis of the 2D unit cell. The inequivalence of the two columns in a projection on the short side of the unit cell may, for example, be caused by differences in the side chain orientation possibly in conjunction with a displacement from the position in the center of the unit cell in a direction parallel to the short axis of the unit cell.

Despite the molecular tilt of 49° , the HBC-C8,2 stacks are packed like columns of circular shape in contrast with unsubstituted bulk HBC which packs like elliptically shaped columns. Unsubstituted bulk HBC crystallizes in a monoclinic structure with space group $P2_1/a$ and the unit-cell dimensions $a = 18.4$ Å, $b = 5.1$ Å, $c = 12.9$ Å, and $\beta = 112.57^\circ$.²¹ Describing unsubstituted bulk HBC by a quasi-rectangular 2D cell results only in a 1.7° deviation from 90° but a long unit-cell axis which is 2.6 times longer than the short axis which is a significantly larger ratio than the factor of $\sqrt{3} \approx 1.7$ for HBC-C8,2. The reason for this difference may, for example, be the tilt direction of the HBC-C8,2 columns or the interdigitation of the alkyl side chains.

Three Phases. The information about the 2D unit cell and the symmetry properties described so far apply to all three HBC-

Table 1. Observed Peak Positions in Reciprocal Å for the Three HBC-C8,2 Phases^a

(h, k, l) [Å ⁻¹]	assignment
(0.129, 0.000, 0.356)*	HBC $_{19.1^\circ}$ (002)
(0.258, 0.000, 0.716)*	HBC $_{19.1^\circ}$ (004)
(0.398, 0.002, 1.095)	HBC $_{19.1^\circ}$ (006)
(0.498, -0.001, 1.392)	HBC $_{19.1^\circ}$ (008)
(0.305, 0.000, 0.117)*	HBC $_{19.1^\circ}$ (100)
(0.610, 0.000, 0.236)	HBC $_{19.1^\circ}$ (200)
(0.477, 0.001, 0.432)	HBC $_{19.1^\circ}$ (103)
(0.256, 0.000, 1.314)*	HBC $_{19.1^\circ}$ (206)
(0.375, 0.000, 0.000)	HBC $_0^\circ$ (002)
(0.783, 0.000, 0.000)	HBC $_0^\circ$ (004)
(0.000, 0.000, 0.302)	HBC $_0^\circ$ (100)
(0.000, 0.000, 0.603)	HBC $_0^\circ$ (200)
(0.000, 0.000, 1.270)	HBC $_0^\circ$ (400)
(1.101, 0.000, 0.638)*	HBC $_0^\circ$ (206), overlap with PTFE peak
(0.291, 0.000, 0.205)	HBC $_{35.2^\circ}$ (002)
(0.647, 0.000, 0.400)	HBC $_{35.2^\circ}$ (004)
(0.177, 0.000, 0.252)*	HBC $_{35.2^\circ}$ (100)
(0.405, 0.000, 0.510)	HBC $_{35.2^\circ}$ (200)
(0.711, 0.000, 0.985)	HBC $_{35.2^\circ}$ (400)

^a The indices in the column "assignment" are given for a unit cell where the short axis of the intercolumnar length L is probed by the 100 reflection and the long axis of the unit cell with the length $\sqrt{3}L$ is probed by the 001 reflection. The peak positions at which the highest intensities were observed are marked with an asterisk

C8,2 phases. The major difference among them is the orientation of the 2D unit cell with respect to the PTFE substrate: The HBC $_0^\circ$ phase has its long 2D unit-cell axis parallel to the substrate; for the HBC $_{35.2^\circ}$ phase, this axis has an angle of $\sim 35^\circ$ to the substrate; and for the HBC $_{19.1^\circ}$ phase, the short unit-cell axis has an angle of $\sim 20^\circ$ with respect to the substrate (see Figure 3). We propose that these different orientations of the same basic structure are induced by the PTFE substrate, mainly via molecular epitaxial but also grapho-epitaxial growth, as described in the following. The observed peak positions which lay the basis for this discussion are listed in Table 1.

(1) HBC $_0^\circ$. The HBC $_0^\circ$ phase grows with the long axis of the 2D unit cell parallel to the substrate. The repeat distance of $\sqrt{3}L \approx \sqrt{3}19.8 \text{ Å} \approx 34.3 \text{ Å}$ along the surface fits very well to six interchain PTFE distances with $6 \times 5.7 \text{ Å} = 34.2 \text{ Å}$. Therefore, we propose that this phase grows epitaxial (i.e., commensurate) on the PTFE substrate. In fact, this suggestion is strongly corroborated as, for example, we did not record any reflections for a rotational variant of the HBC $_0^\circ$ phase which has the *short* axis parallel to the substrate. This phase would need to match about three to four PTFE interchain distances (a HBC-C8,2 intercolumnar distance of 19.8 Å divided by a PTFE interchain distance of 5.7 Å is equal to 3.5). This would imply a compression of the HBC-C8,2 intercolumnar distance by 14% or an expansion by 15%, which is energetically highly unfavorable.

(2) HBC $_{19.1^\circ}$. For the HBC $_{19.1^\circ}$ phase, the short axis of the 2D unit cell has an angle of $\sim 20^\circ$ with respect to the surface and the intercolumnar distance L found is approximately 19.2 Å. If the (105) plane is assumed to be parallel to the surface, the precise tilt angle should be $\arctan(\sqrt{3}/5) \approx 19.1^\circ$ and the repeat distance along the surface $2\sqrt{7}L \approx 102 \text{ Å}$. This corresponds to 18 PTFE interchain distances ($18 \times 5.7 \text{ Å} = 102.6 \text{ Å}$). Therefore, we propose that this phase grows as the HBC $_0^\circ$ phase via molecular epitaxy, too [Note, if an HBC-C8,2 molecule is in the center of the 2D unit cell then the repeat

distance along the surface is $\sqrt{7}L \approx 51 \text{ \AA}$ corresponding to nine PTFE interchain distances].

(3) **HBC_{35.2°}**. For the third phase, we find an intercolumnar distance of $L \approx 20.4 \text{ \AA}$ and an angle of $\sim 35^\circ$ between the long 2D unit-cell axis and the substrate. The repeat distance of $2\sqrt{9}L \approx 2 \times 195 \text{ \AA}$ calculated for an angle of $30^\circ + \arctan(\sqrt{3}/19) \approx 35.2^\circ$ corresponds to 2×34 interchain distances [if an HBC-C8,2 molecule is in the center of the 2D unit cell, then the factor of 2 can be omitted]. The angle between the HBC-C8,2 columns and the PTFE substrate is, however, only 5° . It seems to be unlikely that nucleation on a molecularly flat substrate causes epitaxial growth under such a shallow angle, and with such a long repeat distance. Nevertheless, we observe strong intensity at the corresponding peak positions, which indicates the presence of this phase. Thus, we suggest that, in a grapho-epitaxial growth mode, the nucleation takes place at step edges and other irregularities (as indicated in Figure 3c). Accordingly, it seems to be likely that once the growth of the HBC_{35.2°} phase is started under this shallow angle, it continues epitaxially on the molecularly flat areas of the PTFE film.

Epitaxial Growth. To summarize the proposed growth modes, all three phases observed, which are essentially three orientations of the same basic structure, grow at least 1D epitaxial with the PTFE substrate. Even the proposed grapho-epitaxial nucleation for one of the phases leads to an orientation which allows epitaxial growth. Absolute values for the relative abundances of the three phases cannot be deduced from our data, but it can be stated that HBC_{19.1°} is the predominant phase.

If one tries to find suitable orientations of the observed HBC-C8,2 unit cell which allow commensurate growth on a PTFE substrate, then additionally, to the observed HBC_{0°} and HBC_{19.1°} phase, only an HBC_{13.9°} and HBC_{10.9°} phase seem to be reasonable with respect to the repeat distance along the surface and angle of the unit cell with respect to the surface. The fact that i) two out of four possible epitaxial orientations (HBC_{0°}, HBC_{19.1°}) are observed, and ii) that for the two phases, which are already less probable because of their more shallow angle to the surface (HBC_{13.9°}, HBC_{10.9°}) no diffraction peaks were recorded, underlines the importance of epitaxial growth for the structure of the HBC-C8,2 film.

Crystalline Quality: PTFE. To estimate the long-range order, that is, the crystalline quality of the HBC-C8,2 films, we first briefly characterized the PTFE substrate, since it is unlikely that the epitaxially grown thin film is significantly more ordered than the substrate. The peak corresponding to the 19.5 \AA distance along the 15/7 helices²² is not sufficiently well-defined to be measured accurately, whereas the peak corresponding to the 1.30 \AA distance between two CF₂ groups along the chains is intense and well-defined with a full width at half-maximum (fwhm_ω) of 0.6° . The peak width in degrees can be converted to a peak width q in \AA^{-1} , and using the relationship $l = 2\pi/q$, it is possible to obtain a rough estimate of the correlation length l . For example, the fwhm_ω of 0.6° for the CF₂ distance converts to $l = 130 \text{ \AA}$. For a single crystalline material, this would be the key value to estimate its crystalline quality. For friction-transferred PTFE, this seems not to be the case, since the sliding direction of the PTFE rod, which is probably not completely straight, determines the molecular

alignment. If one hypothetically assumes the alignment of a perfect PTFE layer along a slightly curved line, then the sample rotation scan probes almost exclusively the curvature of this alignment direction. Depending on the sample rotation, different regions of the sample are probed which fulfill the scattering condition determined by the incident beam and the detector position. In this example, a detector rotation scan gives an estimate of the size of the region in which the PTFE molecules are sufficiently straight to scatter coherently. Therefore, the peaks probed seem to be much more narrow in detector scans than in sample rotation scans, which is contrary to the standard relationships between peak widths for single-crystalline material. We do indeed observe that, for example, the CF₂ peak is more narrow in a detector scan than in the sample rotation scan. The detector scan has a fwhm of only 0.4° and a box-function-like peak shape indicative of the true width being even smaller.

The results show that the PTFE substrate is exhibiting long-range ordering but that a quantification of the order has a high uncertainty because of the curvature along the sliding direction of the PTFE rod and thereby along the molecular axis. The observed peak widths stay well below the 6° fwhm of the orientational distribution determined for friction-transferred PTFE films which are prepared by dragging a PTFE rod twice over a glass substrate to obtain a larger film.²³ One should generally keep in mind that, above 19°C , PTFE lacks long-range order along the chain axis which explains why the peak corresponding to the 19.5 \AA distance along the 15/7 helices is so much less well-defined than the peak corresponding to the distance between the CF₂ subunits along the same direction. The PTFE configuration may be different in friction-transferred layers compared to bulklike PTFE material.²⁴ This could explain the spread of the PTFE inter- and intramolecular distances which are reported in the literature.^{25,22,3,7,24}

Crystalline Quality: HBC-C8,2. The HBC-C8,2 peaks are broader in the sample rotation scans than in the corresponding detector scans. This is in line with epitaxial growth along the PTFE substrate that we found to be aligned in an almost straight manner. According to this argumentation, the most narrow HBC-C8,2 peaks cannot have a smaller fwhm than the PTFE substrate peaks. For example, the HBC_{19.1°}(100) peak shown in Figure 4 has a fwhm_ω of 1.7° . The observed fwhm values are extraordinarily good for organic materials. They are comparable to those observed for typical metal crystals such as copper. As described above, a quantification has a high uncertainty and should therefore be avoided.

The size of the areas which scatter coherently does not necessarily reflect the charge carrier mobility along the HBC-C8,2 columns. For example, the liquid crystalline D_h phase displays still high (intrinsic) charge carrier mobilities despite its higher molecular disorder compared to the crystalline phase. High crystalline quality is generally believed to lead to high mobilities. However, in the case of the aligned films described in this article we believe domain boundaries to be larger barriers for the charge carriers than disorder along the HBC-C8,2 columns.

Quasi-2D Growth. Above 19° , PTFE ceases to be well-ordered along the molecular chains. Hence, long-range epitaxial

(22) Young, R. J.; Lovell, P. A. *Introduction to Polymers*; Chapman & Hall: London, 1991; Chapter 4, pp 249–251.

(23) Tanigaki, N.; Yoshida, Y.; Kaito, A.; Yase, K. *J. Polym. Sci., Part B: Polym. Phys.* **2001**, *39*, 432–438.

(24) Dietz, P.; Hansma, P. K.; Ihn, K. J.; Motamedi, F.; Smith, P. J. *Mater. Sci.* **1993**, *28*, 1372–1376.

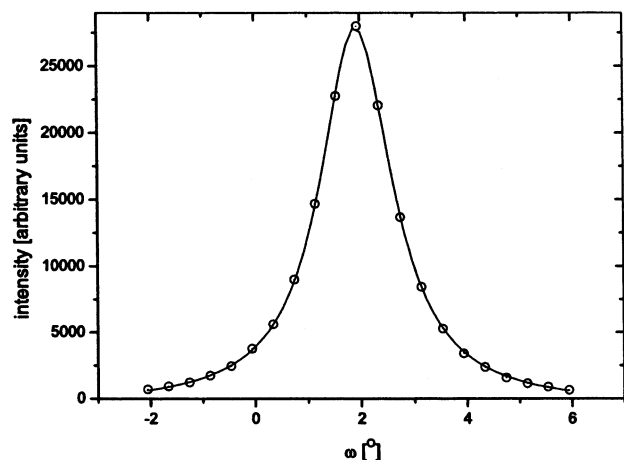


Figure 4. Sample rotation scan (rocking curve) of the HBC_{19,1°} (100) peak. The full width at half-maximum is $\sim 1.7^\circ$.

order is unlikely to occur in this direction, but rather, a quasi-2D growth mode is expected and indeed found for a number of systems. In the Introduction, it was mentioned that vacuum deposited diazo-dyes^{10,11} and tris(8-hydroxyquinoline) aluminum(III)¹² grow on friction-transferred PTFE in a way which suggests at least a 1D epitaxy mechanism. For different *n*-alkanes on PTFE, a strong dependence of the orientation mechanism on the *n*-alkane chain length has been found. An epitaxy mechanism based on the formation of short-range intermolecular interactions with the oriented polymer chains has to be invoked to explain the alignment of alkane molecules on the substrates.²⁶ These previously reported results and the current findings strongly support that many thin films grow in a mode with a strong 1D epitaxy perpendicular to the PTFE chains and further alignment along the polymer molecules. Therefore, the growth mode can be described as quasi-2D. The order and growth in the third dimension are determined by interactions within the thin film but enhanced indirectly by the PTFE layer, since a quasi-2D ordered substrate is a good premise for 3D ordered growth.

Invoking this quasi-2D growth mechanism, minor changes, for example, in the chemical structure of the adsorbed molecules, may have a pronounced influence on the nucleation and ordering of the film. Therefore, *n*-alkanes may easily exhibit different ordering mechanisms, depending on their chain length, and therefore, probably only those orientational variances of the basic HBC-C8,2 structure occur, which allow epitaxial growth on the PTFE substrate. The same argument can explain the tilt of 33° of the molecular planes with respect to the substrate in the structure of sexithiophene thin films deposited on a PTFE alignment layer²⁷ and also the selection of azimuthal orientations in the growth of tris(8-hydroxyquinoline) aluminum(III) on PTFE¹² and the strong dependence of the orientational ordering of diazo-dyes on their molecular structure fits into this category.¹⁰

Improving the Crystalline Quality. Even when all the three HBC-C8,2 phases are highly oriented, it will be crucial to reduce

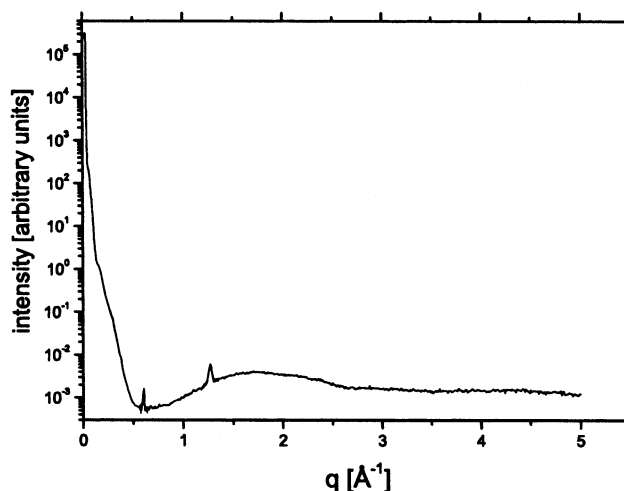


Figure 5. A specular (00*l*) rod (also called $\Theta-2\Theta$ scan) of HBC-C8,2/PTFE. The two crystalline peaks are associated with the HBC_{0°} phase.

the number of coexisting phases in order to enhance the device performance of hexabenzocoronene transistors further. On the basis of the described quasi-2D epitaxial growth mode, we propose that the occurrence of rotational variants can be significantly influenced by changing the length of the peripheral substituents and thereby changing the intercolumnar distance *L*.

For systems such as HBC-C8,2/PTFE, where one phase is predominant, it is promising to steer the thin film more toward its equilibrium state. This can be done by minimizing kinematic effects while the film is grown. Other possibilities are annealing techniques such as temperature or solvent vapor annealing applied after the film has been grown.

Suitable Characterization Techniques. Concerning suitable techniques to study thin films with a complex structure, we would like to point out that standard X-ray diffraction $\Theta-2\Theta$ scans and transmission electron diffraction at normal incidence do not reveal the full 3D structural information and can therefore be very misleading if one tries to judge the crystalline quality of the sample. This is evidently the case for the thin film system described in this paper, as shown in Figure 5. The (00*l*) rod scan shown in this figure corresponds to a standard $\Theta-2\Theta$ scan which is usually performed to characterize a thin film using X-rays. Only peaks corresponding to the HBC_{0°} phase, which has a low index plane parallel to the surface, can be seen in this intensity profile. The HBC_{19,1°} and the HBC_{35,2°} phase have no low index plane parallel to the surface and can therefore not be detected. It is advisable to exploit the free parameters given by the sample orientation to lower the possibility of missing the strong intensity at (*hkl*)-peak positions which are neither in plane with $l \approx 0$ (transmission electron diffraction) nor specularly out of plane with $h = k = 0$ (standard X-ray diffraction). To characterize these more complex systems, a nondestructive full 3D technique like surface X-ray diffraction is necessary. This technique is however time-consuming, and the use of synchrotron radiation is very often required; the sample throughput is therefore limited.

Conclusion and Outlook

We succeeded in producing well-ordered and uniaxially aligned HBC-C8,2 films from solution by crystallization on friction-transferred PTFE layers.

- (25) Kerbow, D. L.; Sperati, C. A. *Physical Constants of Fluoropolymers*. In *Polymer handbook*, 3rd ed.; Brandrup, J., Immergut, E. H., Eds.; John Wiley and Sons: New York, 1989; Chapter V, pp 31–45.
- (26) Damman, P.; Fischer, C.; Krüger, J. K. *J. Chem. Phys.* **2001**, *114*, 8196–8204.
- (27) Wittmann, J. C.; Straupé, C.; Meyer, S.; Lotz, B.; Lang, P.; Horowitz, G.; Garnier, F. *Thin Solid Films* **1998**, *333*, 272–277.

Peaks corresponding to three crystalline HBC-C8,2 majority phases were observed. The three phases have the same basic structure but three different rotational orientations. Each phase consists of HBC-C8,2 columns running parallel to the PTFE chains of the substrate. Along the columns, the molecules are tilted by $\sim 49^\circ$. The coexistence of these phases may explain the discrepancy of the field-effect mobility ($\mu_{\parallel} \leq 10^{-3} \text{ cm}^2 \text{ V}^{-1} \text{ s}^{-1}$) to the intrinsic mobility ($\mu_{\text{intrinsic}} \approx 0.4 \text{ cm}^2 \text{ V}^{-1} \text{ s}^{-1}$), as determined by pulse-radiolysis time-resolved microwave conductivity measurements.

A quasi-2D epitaxial growth mechanism (with a grapho-epitaxial component for one of the three phases) is invoked to explain the formation of the three rotational HBC-C8,2 variants. The quasi-2D mechanism may as well explain many other findings reported in the literature for thin films grown on PTFE.

It is proposed that changing the hydrocarbon chain length of the peripheral HBC substituents is promising for steering the system into only one crystalline phase, which would be highly desirable to increase the already high charge carrier mobilities closer toward the intrinsic value.

Standard $\Theta-2\Theta$ X-ray diffraction and transmission electron diffraction at normal incidence can be very misleading tools to estimate the crystalline order in a thin film of complex structure.

Acknowledgment. We would very much like to express our thanks to Klaus Müllen and co-workers for providing us with the HBC material. Also, we would like to acknowledge Paul Smith for helpful discussions and the use of the Tribotrak apparatus, John M. Warman and Melissa Sharp for helpful discussions, and the HASYLAB staff for practical assistance during the surface X-ray diffraction experiments. M.M.N. and O.B. would like to thank DanSync for financial support. A.M.C. would like to acknowledge the European Commission for financial support by means of a Marie Curie Fellowship, Contract Number HPMF-CT-2000-00737. N.S. would like to express thanks to the Swiss National Science Foundation for a young researchers grant. Research reported in this article is part of a network called DISCEL and financed by the European Commission, Contract Number G5RD-CT-2000-00321.

JA028509C